Supplementary Material

Anatomical landmarks for ROIs

Coordinates for left and right M1 were obtained from the 'Tapping' condition, with local maxima at the 'hand knob' formation of the precentral gyrus (Yousry et al., 1997). For the premotor ROIs of PMC and SMA, we computed a conjunction analysis across all four conditions, ensuring that the regions were not only activated in the higher motor control conditions, but also in the localizer task. The SMA was located on the mesial cortical surface anterior to the paracentral lobule, superior to the cingulate sulcus and posterior to the coronal plane running through the anterior commissure (y coordinate ≤ 0, (Picard and Strick, 2001). Hence, we deliberately chose the caudal parts of SMA, i.e., SMA proper, instead of pre-SMA because of the strong BOLD activation in this region induced by our task, knowledge about structural connectivity from non-human primate studies (Rouiller et al., 1994) and experience in motor network connectivity based on previous studies using DCM (Boudrias et al., 2012; Grefkes et al., 2010; Pool et al., 2013). The PMC was located at the intersection of the superior branch of the precentral sulcus and the superior frontal sulcus (Picard and Strick, 2001). Hence, this region most likely reflects a subregion of the PMC with strong functional coupling with both medial IPS and PFC (see a recent meta-analysis by (Genon et al., 2016). This region is particularly important for both top-down/goal-driven processes and bottom-up integration of visuospatial information into motor plans (Abe and Hanakawa, 2009; Luppino et al., 2003). When referring to non-human primates, this ROI most likely reflects area F2vr (Boussaoud, 2001; Genon et al., 2016). Importantly, there was explicitly no overlap with the ROI used for primary motor cortex. For the IPS ROI we chose its anterior and medial portion, i.e., a region devoted to visuomotor integration and coordinate transformation, most likely referring to the MIP in non-human primates (Grefkes and Fink, 2005; Grefkes et al., 2004). This regions has strong structural and functional connectivity in monkeys and humans with premotor regions and is crucially involved in visuomotor transformation processes (Grefkes et al., 2004). Coordinates of all ROIs are provided in the Supplementary Table 1.

Supplementary Table 1

	x-coordinate	y-coordinate	z-coordinate
PFC-L	-36.4 ± 4.3	36.3 ± 6.5	27.1 ± 5.4
PFC-R	34.1 ± 6.2	39.7 ± 4.6	26.8 ± 4.3
SMA	0.0 ± 2.8	-4.4 ± 3.4	60.8 ± 5.6
PMC-L	-35.6 ± 5.3	-7.9 ± 3.5	60.7 ± 3.7
PMC-R	37.2 ± 6.0	-5.5 ± 5.4	60.3 ± 5.2
M1-L	-36.8 ± 3.1	-24.1 ± 3.1	60.8 ± 6.0
M1-R	37.8 ± 3.5	-23.8 ± 3.1	60.7 ± 6.0
IPS-L	-32.1 ± 5.1	-51.3 ± 5.9	47.6 ± 5.0
IPS-R	34.3 ± 4.1	-55.8 ± 6.3	46.9 ± 5.1

ROI coordinates for the DCM analysis
Mean MNI coordinates (x, y, z) for all ROIs across all subjects, n=24. PFC = prefrontal cortex, PMC = premotor cortex, SMA = supplementary motor area, M1 = primary motor cortex, IPS = intraparietal sulcus. L = left-hemispheric ROIs, R = right-hemispheric ROIs.

Supplementary Figure 1
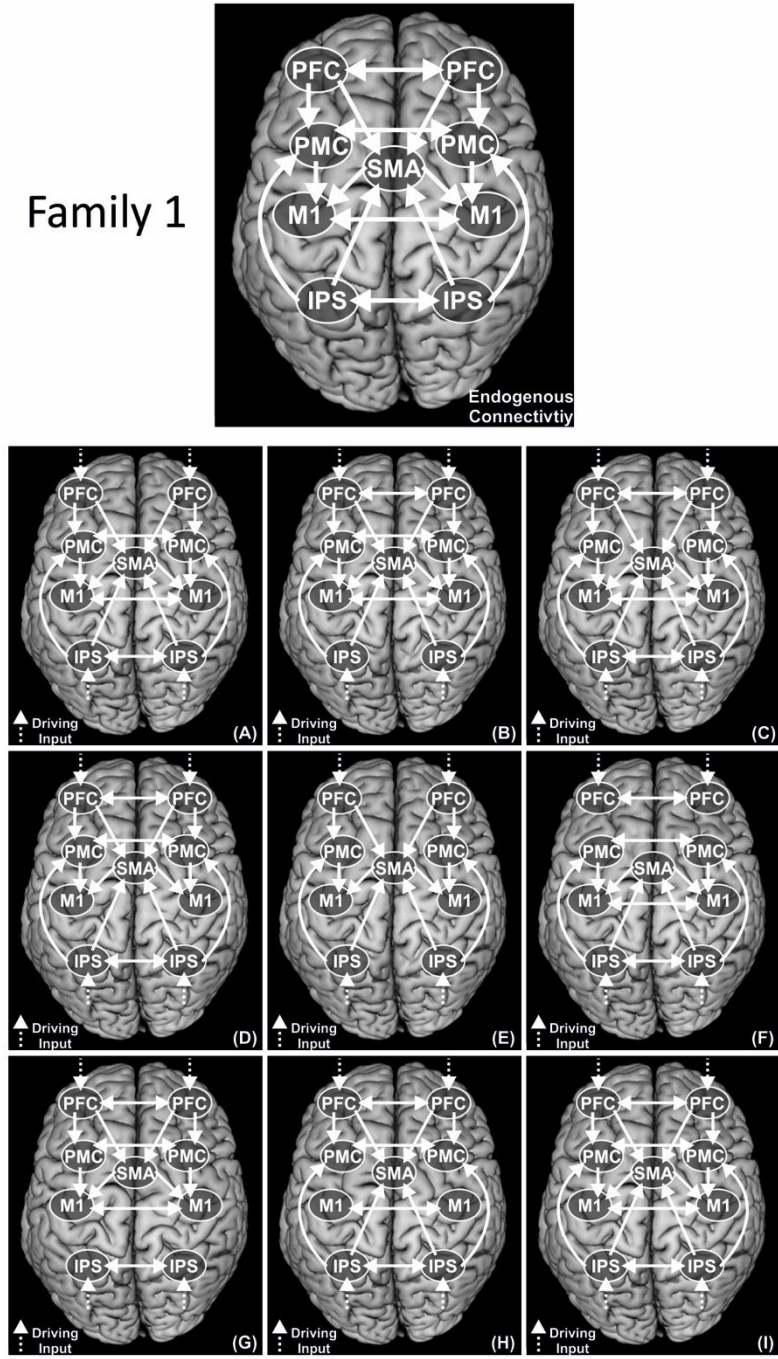
Model space Family 1 (including PFC-premotor modulation)

All models within Family 1 shared the same endogenous network connectivity matrix (DCM-A) and varied in complexity regarding condition-dependent modulations (DCM-B): (A) without interhemispheric PFC coupling, (B) without interhemispheric IPS coupling, (C) without interhemispheric PMC coupling, (D) without interhemispheric M1 coupling, (E) without any interhemispheric coupling, (F) without PFC-premotor coupling, (G) without IPS-premotor coupling, (H) without premotor-M1 coupling, (I) modulation of all endogenous connections.

Supplementary Figure 2
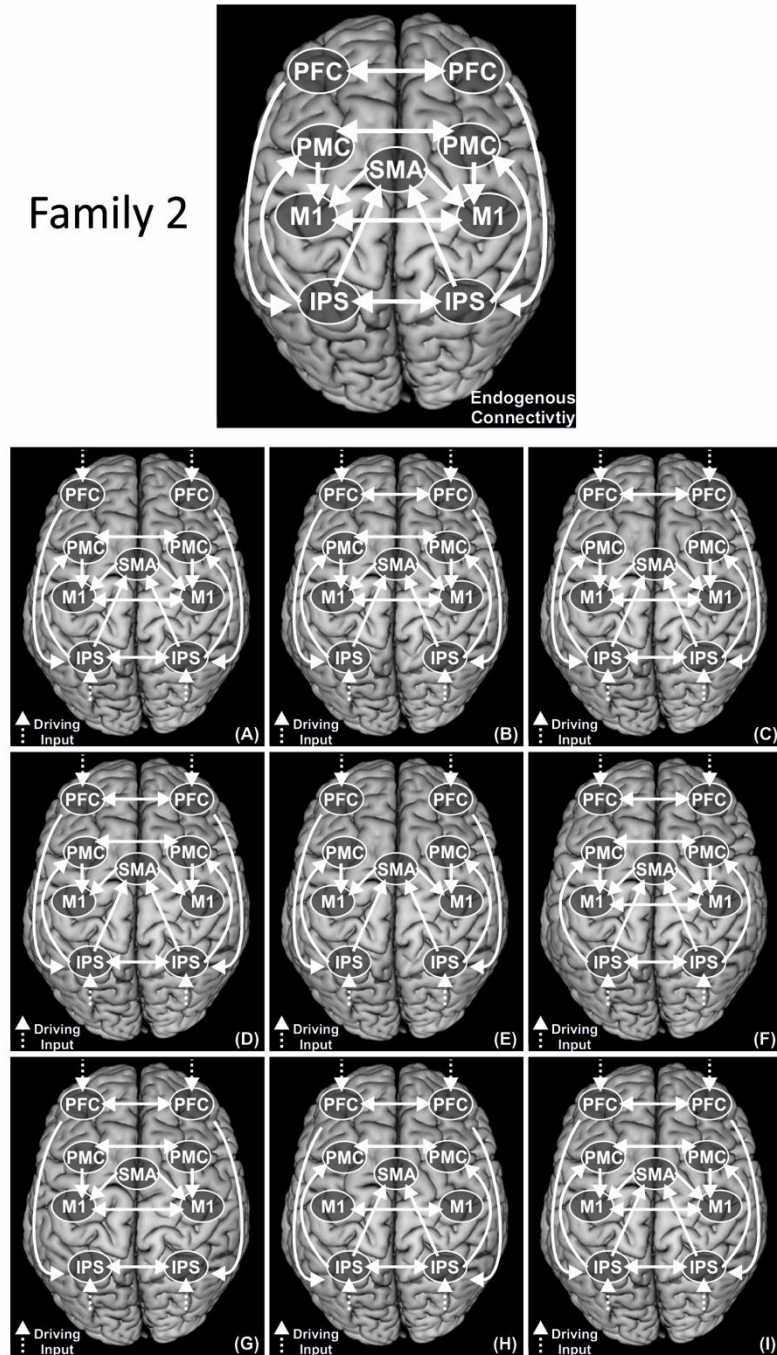
Model space Family 2 (including PFC-IPS modulation)

All models within Family 2 shared the same endogenous network connectivity matrix (DCM-A) and varied in complexity regarding condition-dependent modulations (DCM-B): (A) without interhemispheric PFC coupling, (B) without interhemispheric IPS coupling, (C) without interhemispheric PMC coupling, (D) without interhemispheric M1 coupling, (E) without any interhemispheric coupling, (F) without PFC-IPS coupling, (G) without IPS-premotor coupling, (H) without premotor-M1 coupling, (I) modulation of all endogenous connections.

Supplementary Figure 3
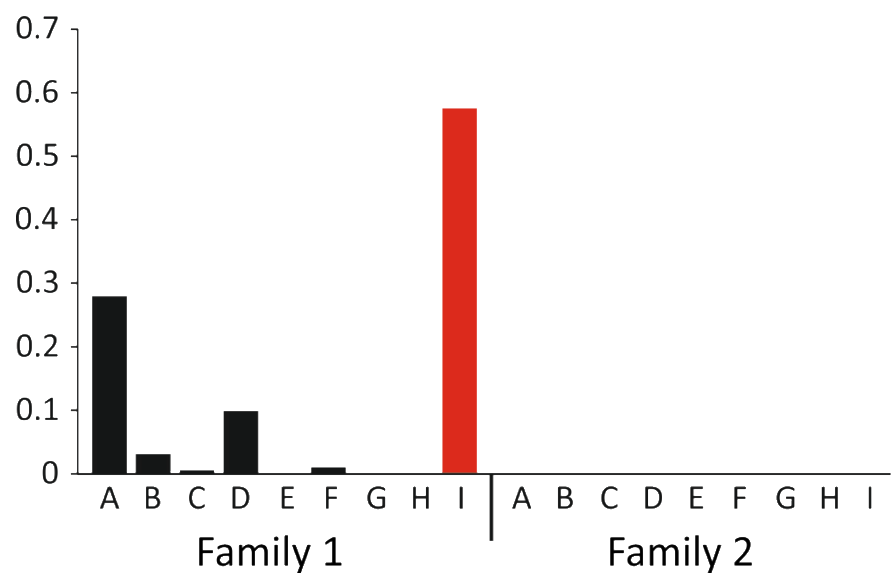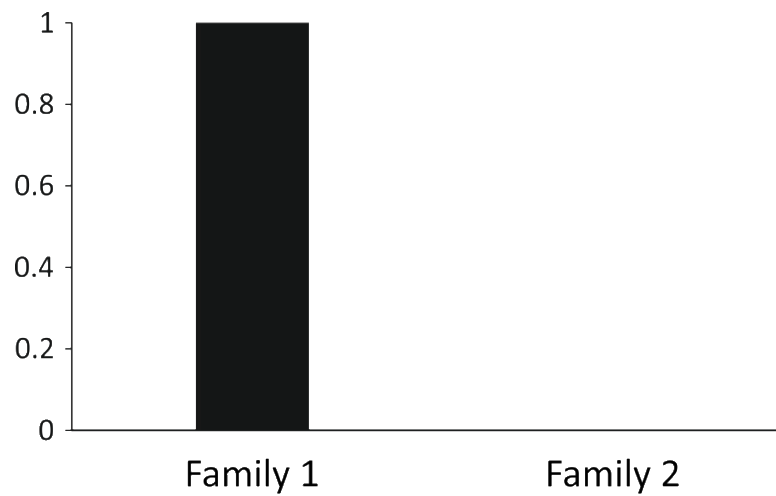

Bayesian model selection

Results of the random-effects Bayesian model selection. Upper panel: Results of the family comparison; Lower panel: The most likely model given the data (I, Family 1) is highlighted in red. Results are shown for the entire sample, i.e., n=24. Note that the model selection procedure revealed the same winning model when testing for each age group separately.

Supplementary Figure 4
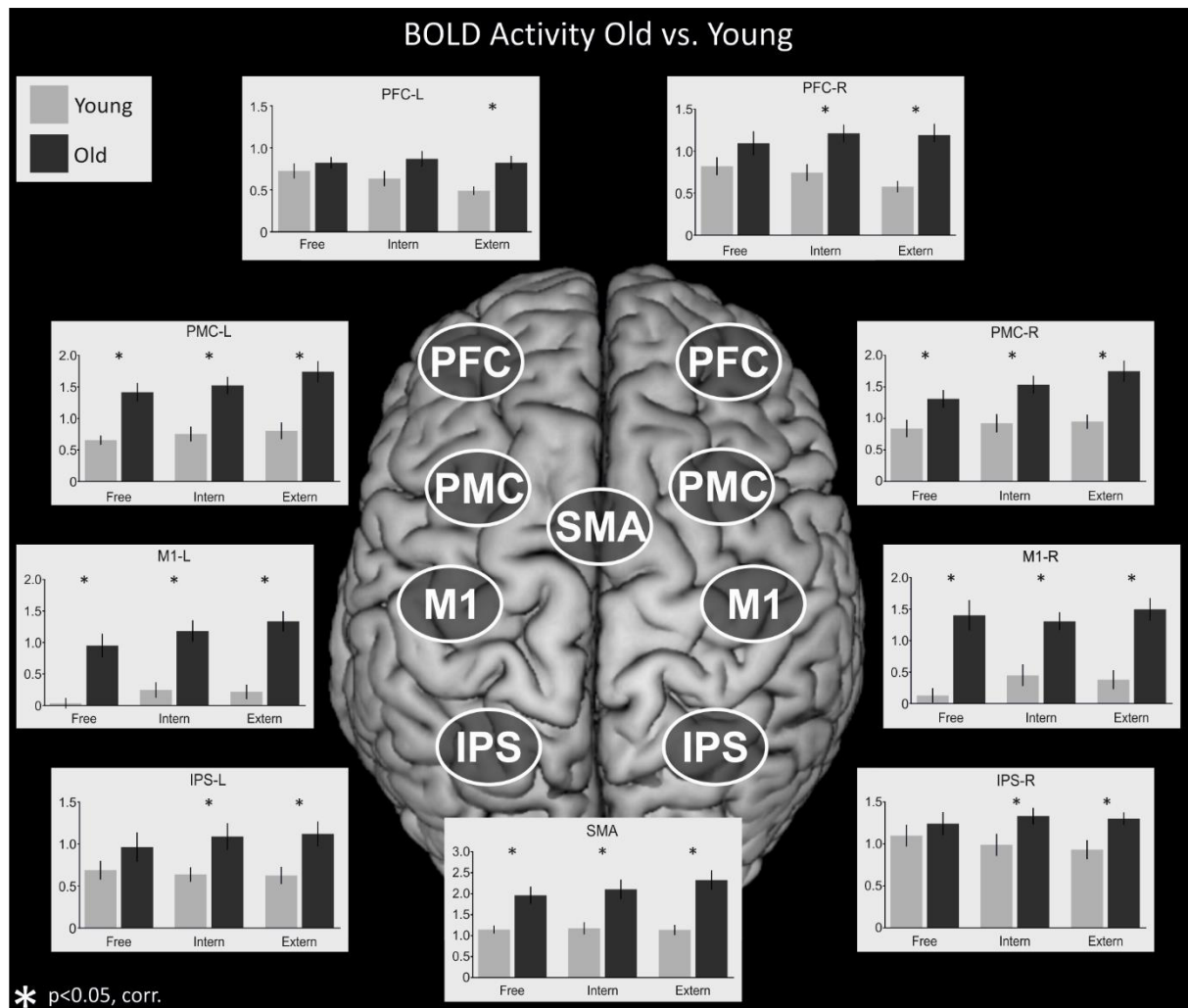
Between-group activity differences for ROI analysis

Note that all differences between groups remained significant when controlling for structural atrophy as informed by the VBM analysis. PFC = prefrontal cortex, PMC = premotor cortex, SMA = supplementary motor area, M1 = primary motor cortex, IPS = intraparietal sulcus. R = right-hemispheric, L = left-hemispheric. p<0.05, FDR-corrected for multiple comparisons. Error bars: SEM.

Supplementary Figure 5
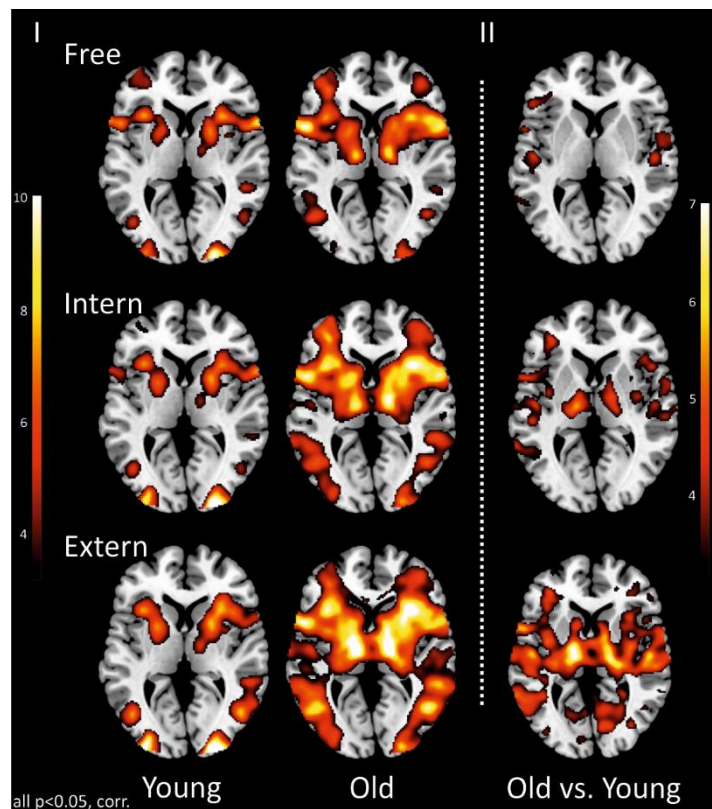
Subcortical BOLD activity

(I) Basal ganglia and thalamus activity for young and older subjects for each condition separately. (II) Significantly enhanced BOLD activity in old as compared to young individuals for each condition separately. All p<0.05, family-wise error (FWE) corrected at the cluster level. Note that at the subcortical level, strongest between group differences were found at the level of the thalamus, especially for the 'Extern' and 'Intern' condition.

Michely et al.: Network connectivity in ageing

'Free'

Coordinates			Side	Region	T-value
x	**y**	**z**			
-35	-23	50	L	Precentral Gyrus, Primary Motor Cortex	7.22
-41	-12	59	L	Precentral Gyrus, Premotor Cortex	6.80
-38	-32	59	L	Postcentral Gyrus, Somatosensory Cortex	6.44
47	-21	11	R	Parietal Operculum	5.53
47	-26	57	R	Postcentral Gyrus, Somatosensory Cortex	5.49
-45	6	14	L	Inferior Frontal Gyrus, Pars opercularis	5.43
38	-15	60	L	Precentral Gyrus, Premotor Cortex	5.42
38	-26	63	R	Precentral Gyrus, Primary Motor Cortex	5.31
35	-38	-23	R	Cerebellum	5.27
-3	-9	60	L	Posterior-Medial Frontal Gyrus, SMA	5.04
-50	-23	14	L	Rolandic Operculum	4.81
-23	-48	72	L	Superior Parietal Lobule	4.76
-12	0	44	L	Midcingulate Cortex	4.74
-60	-30	23	L	Inferior Parietal Lobule	4.64
8	-6	47	R	Posterior-Medial Frontal Gyrus, pre-SMA	4.64
6	-8	59	R	Posterior-Medial Frontal Gyrus, SMA	4.58
-18	-56	-18	L	Cerebellum	4.49
57	-29	12	R	Superior Temporal Gyrus	4.47
-57	-56	0	L	Middle Temporal Gyrus	4.37
15	-21	66	R	Precentral Gyrus, Premotor Cortex	4.30
9	3	32	R	Midcingulate Cortex	4.25
-51	30	6	L	Inferior Frontal Gyrus, Pars triangularis	4.24
53	2	8	R	Rolandic Operculum	4.21
63	-21	23	R	Supramarginal Gyrus	3.83
-39	36	17	L	Middle Frontal Gyrus	3.79
-35	41	-9	L	Middle Orbital Gyrus	3.73

'Intern'

Coordinates			Side	Region	T-value
x	y	z			
33	-23	48	L	Precentral Gyrus, Primary Motor Cortex	6.85
-41	-11	57	L	Precentral Gyrus, Premotor Cortex	6.58
35	-32	59	L	Postcentral Gyrus, Somatosensory Cortex	5.95
-5	-8	62	L	Posterior-Medial Frontal Gyrus, SMA	5.90
54	-32	12	R	Superior Temporal Gyrus	5.89
-20	-62	-15	L	Cerebellum	5.75
9	-6	59	R	Posterior-Medial Frontal Gyrus, SMA	5.61
36	41	11	R	Middle Frontal Gyrus	5.61
-15	-15	5	L	Thalamus	5.57
-36	20	-15	L	Inferior Frontal Gyrus, Pars orbitalis	5.55
24	-29	71	R	Precentral Gyrus, Primary Motor Cortex	5.51
-11	5	45	L	Midcingulate cortex	5.45
-32	39	14	L	Middle Frontal Gyrus	5.37
12	-14	42	R	Midcingulate cortex	5.29
-45	6	14	L	Inferior Frontal Gyrus, Pars opercularis	5.21
14	-9	0	R	Thalamus	5.15
29	-41	65	R	Postcentral Gyrus, Somatosensory Cortex	5.14
-27	-42	41	L	Intraparietal Sulcus	5.14
3	-89	23	R	Cuneus	4.66
32	-56	33	R	Intraparietal Sulcus	4.65
-42	-68	-9	L	Inferior Occipital Gyrus	4.64
29	-56	-26	R	Cerebellum	4.59
21	-48	68	R	Superior Parietal Lobule	4.40
-30	57	65	L	Superior Parietal Lobule	4.37
-66	-48	3	L	Middle Temporal Gyrus	4.26
39	38	32	R	Middle Frontal Gyrus	3.90
-45	24	32	L	Middle Frontal Gyrus	3.65

'Extern'

Coordinates			Side	Region	T-value
x	y	z			
-35	-21	47	L	Precentral Gyrus, Primary Motor Cortex	8.12
-41	-11	57	L	Precentral Gyrus, Premotor Cortex	7.85
-20	-60	-15	L	Cerebellum	7.48
-15	-17	2	L	Thalamus	7.46
32	-50	-21	R	Cerebellum	6.91
-53	-63	-6	L	Inferior Temporal Gyrus	6.64
-57	8	9	L	Inferior Frontal Gyrus, Pars opercularis	6.61
-12	2	44	L	Midcingulate cortex	6.51
8	-2	-3	R	Thalamus	6.49
-33	-30	56	L	Postcentral Gyrus, Somatosensory Cortex	6.47
-3	-8	62	L	Posterior-Medial Frontal Gyrus, SMA	6.43
-44	-33	18	L	Inferior Parietal Lobule	6.37
56	-24	8	R	Superior Temporal Gyrus	6.36
6	-5	45	R	Posterior-Medial Frontal Gyrus, pre-SMA	6.35
5	-15	72	R	Posterior-Medial Frontal Gyrus, SMA	6.34
36	41	11	R	Middle Frontal Gyrus	6.32
-33	15	-9	L	Insula	6.30
-35	30	11	L	Inferior Frontal Gyrus, Pars triangularis	6.19
27	-29	62	R	Precentral Gyrus, Primary Motor Cortex	6.02
-30	-57	65	L	Superior Parietal Lobule	5.54
-38	36	18	L	Middle Frontal Gyrus	5.46
32	-56	33	R	Intraparietal Sulcus	5.42
30	-41	63	R	Postcentral Gyrus, Somatosensory Cortex	5.35
8	6	33	R	Midcingulate Cortex	5.34
23	-57	68	R	Superior Parietal Lobule	5.02
36	23	32	R	Middle Frontal Gyrus	4.54
-24	-60	38	L	Intraparietal Sulcus	4.23

Local maxima of overactivation in old vs. young subjects (whole-brain analysis)
(P<0.05, FWE corrected at the cluster level), L = left, R = right

References

Abe, M., Hanakawa, T. 2009. Functional coupling underlying motor and cognitive functions of the dorsal premotor cortex. Behav Brain Res 198, 13-23.

Boudrias, M.H., Goncalves, C.S., Penny, W.D., Park, C.H., Rossiter, H.E., Talelli, P., Ward, N.S. 2012. Age-related changes in causal interactions between cortical motor regions during hand grip. Neuroimage 59, 3398-3405.

Boussaoud, D. 2001. Attention versus intention in the primate premotor cortex. Neuroimage 14, S40-45.

Genon, S., Li, H., Fan, L., Muller, V.I., Cieslik, E.C., Hoffstaedter, F., Reid, A.T., Langner, R., Grefkes, C., Fox, P.T., Moebus, S., Caspers, S., Amunts, K., Jiang, T., Eickhoff, S.B. 2016. The Right Dorsal Premotor Mosaic: Organization, Functions, and Connectivity. Cereb Cortex.

Grefkes, C., Fink, G.R. 2005. The functional organization of the intraparietal sulcus in humans and monkeys. J Anat 207, 3-17.

Grefkes, C., Ritzl, A., Zilles, K., Fink, G.R. 2004. Human medial intraparietal cortex subserves visuomotor coordinate transformation. Neuroimage 23, 1494-1506.

Grefkes, C., Wang, L.E., Eickhoff, S.B., Fink, G.R. 2010. Noradrenergic modulation of cortical networks engaged in visuomotor processing. Cereb Cortex 20, 783-797.

Luppino, G., Rozzi, S., Calzavara, R., Matelli, M. 2003. Prefrontal and agranular cingulate projections to the dorsal premotor areas F2 and F7 in the macaque monkey. Eur J Neurosci 17, 559-578.

Picard, N., Strick, P.L. 2001. Imaging the premotor areas. Curr Opin Neurobiol 11, 663-672.

Pool, E.M., Rehme, A.K., Fink, G.R., Eickhoff, S.B., Grefkes, C. 2013. Network dynamics engaged in the modulation of motor behavior in healthy subjects. Neuroimage 82, 68-76.

Rouiller, E.M., Babalian, A., Kazennikov, O., Moret, V., Yu, X.H., Wiesendanger, M. 1994. Transcallosal connections of the distal forelimb representations of the primary and supplementary motor cortical areas in macaque monkeys. Exp Brain Res 102, 227-243.

Yousry, T.A., Schmid, U.D., Alkadhi, H., Schmidt, D., Peraud, A., Buettner, A., Winkler, P. 1997. Localization of the motor hand area to a knob on the precentral gyrus. A new landmark. Brain 120 (Pt 1), 141-157.